Microporous and Mesoporous Materials 242 (2017) 50–58

Contents lists available at ScienceDirect

Microporous and Mesoporous Materials

journal homepage: www.elsevier.com/locate/micromeso

Microwave-assisted synthesis of magnetic Fe_3O_4-mesoporous magnesium silicate core-shell composites for the removal of heavy metal ions

Zhengfu Zhao [a, 1], Xian Zhang [a, 1], Hongjian Zhou [a, **], Gang Liu [b], Mingguang Kong [a], Guozhong Wang [a, *]

[a] Key Laboratory of Materials Physics, Centre for Environmental and Energy Nanomaterials, Anhui Key Laboratory of Nanomaterials and Nanotechnology, Institute of Solid State Physics, Chinese Academy of Sciences, Hefei 230031, PR China
[b] Institute of Applied Technology, Hefei Institutes of Physical Science, Chinese Academy of Sciences, Hefei 230031, PR China

ARTICLE INFO

Article history:
Received 19 April 2016
Received in revised form
21 December 2016
Accepted 8 January 2017
Available online 9 January 2017

Keywords:
Mesoporous core-shell nanostructures
Microwave-assisted
Toxic metal ions
Competitive adsorption
Magnetic separation

ABSTRACT

An ultrafast and facile microwave assisted hydrothermal approach was applied to synthesize magnetic Fe_3O_4-mesoporous magnesium silicate (FMMS) core-shell composites for effective removal of Cu^{2+}, Cd^{2+} and Pb^{2+} from aqueous solutions. The FMMS composites have mesoporous magnesium silicate shells encapsulated Fe_3O_4 spheres core structures, and the mesoporous shell assembled by a large number of intercrossed nanosheets with a diameter of 4.0 nm pores, thus exhibited the excellent capability to remove Pb^{2+} (223.2 mg/g) and Cu^{2+} (53.5 mg/g) ions from aqueous solutions. The superior removal capacity of the FMMS composites can be ascribed to its mesoporous structures with abundant adsorption active sites. The competitive adsorption studies showed that the adsorbent affinity order of three metal ions by FMMS composites is Cu^{2+}>Pb^{2+}>Cd^{2+}. It is noteworthy that the heavy metal ions could not only adsorb on the surface of FMMS composites, but also intercalate into the intercrossed nanosheets of mesoporous magnesium silicate shell, which reveals the synergistic effect of the electrostatic attraction, surface complexation and ion exchange coupled with the adsorption bonding with surface hydroxyl groups. Furthermore, the FMMS composites exhibited excellent sorption-regeneration performance, which can be easily separated and recovered by external magnet. All results demonstrated that the magnetic FMMS core-shell composite was a promising sorbent material for the preconcentration and separation of heavy metal ions from the waste water.

1. Introduction

Along with the rapid development of modern industry, a large amount of wastes containing heavy metals have been discharged into the environment over the past few decades [1,2]. The contained heavy metals, such as Pb^{2+}, Cd^{2+}, and Cu^{2+} in industrial waste water, can cause serious health problems to animals and human beings [3,4]. Thus, it is necessary and urgent to find effective ways to remove such toxic metal ions from waste water [5]. As an effective approach, the adsorption technique is widely used to remove heavy metal ions from waste water because of its low operational and maintenance costs, convenience, and wide adaptability [6–9]. Accordingly, various nanostructured adsorbents, owe to their unique physical and chemical properties such as large specific surface areas, high adsorption capacity and fast adsorption rate, have been extensively studied for the removal of heavy metal ions and organic pollutants from waste water [10–16]. However, the nanoadsorbents still suffer from practical issues involving the formation of aggregates, difficulties in subsequent separation, regeneration, and recycling processes, which impede their applications [17–19]. Thus, there is an urgent demand to develop novel nanomaterials with sufficient active sites (the ion exchange sites or vacancies) and easy solid-liquid separation capacity in order to rapidly and efficiently remove toxic heavy metal ions for water remediation applications.

* Corresponding author.
** Corresponding author.
E-mail addresses: hjzhou@issp.ac.cn (H. Zhou), gzhwang@issp.ac.cn (G. Wang).
[1] These authors contributed equally to this work.

http://dx.doi.org/10.1016/j.micromeso.2017.01.006
1387-1811/

The silicates as a complicated class of minerals and the richness in crystal structures provide silicates with affluent physical, chemical and materials applications [20–22]. Recently, there has been an upsurge of interest in synthesis of nanostructured silicates with different morphology because of their great potential application in many fields, such as absorbents in water purity, catalyst, molecular sieves, drug delivery, lithium batteries, and gas adsorption and separation [23–28]. Above all, silicates as eco-friendly materials are good adsorbents for the removal of various harmful cations [29–34]. Previously, we reported that silica colloidal spheres were employed as the chemical template (the source of silicate ions) to synthesize magnesium silicate hollow spheres by a facile hydrothermal strategy [35]. The as-synthesized magnesium silicate hollow spheres with large specific surface area exhibited availability for the removal of organic and heavy metal ions efficiently from waste water [19,31]. However, the separation and recycling process is a bottleneck to operate the magnesium silicate hollow spheres for water treatment. Even though the separation is technically available using centrifugation, it takes over 1 h and many additional processes are carried out to make sure complete separation from non-binding materials [12,30,36,37]. Therefore, rapid magnetic separative nanoadsorbent has became increasingly significance for practical implementation of waste water treatment [36–39].

In this paper, we developed an ultrafast and facile microwave assisted hydrothermal approach to synthesize magnetic Fe_3O_4-mesoporous magnesium silicate (FMMS) core-shell composites composed of magnetite core and mesoporous magnesium silicate shell. The magnetic FMMS core-shell composites as a novel adsorbent were investigated their adsorption kinetics, isotherms, and adsorption thermodynamic for the removal of Pb^{2+}, Cu^{2+} and Cd^{2+} from aqueous solutions. Moreover, the competitive adsorption performance of the FMMS composites for the Pb^{2+}, Cu^{2+} and Cd^{2+} toxic ions were also studied to evaluate their adsorbent affinity for three metal ions. In addition, mechanism for the removal of heavy metal ions by the FMMS composites was also discussed. The FMMS composites can be easily separated from the wastewater by using a magnet and have the excellent reusability, which would be a promising micro/nanostructured adsorbent for removal of heavy metal ions in industrial waste water.

2. Experimental section

2.1. Material

Hexahydrated ferric chloride ($FeCl_3 \cdot 6H_2O$), hexahydrated magnesium chloride ($MgCl_2 \cdot 6H_2O$), ammonium chloride (NH_4Cl), ammonia water ($NH_3 \cdot H_2O$), tetraethyl orthosilicate (TEOS), sodium acetate, polyethylene glycol (PEG200), lead nitrate ($Pb(NO_3)_2$), cadmium nitrate ($Cd(NO_3)_2$) and trihydrated copper nitrate ($Cu(NO_3)_2 \cdot 3H_2O$) were purchased from Sinopharm Chemical Reagent Co. Ltd, Shanghai, China. All these chemicals were analytical grade and used without further purification. Deionized water was used throughout the experiments.

2.2. Synthesis of magnetic FMMS core-shell composites

The unique magnetic FMMS core-shell composites with magnetic cores and hierarchical magnesium silicate shells were fabricated through a two-step method. Firstly, the magnetic particles (Fe_3O_4) were prepared by means of a solvothermal reaction as reported previously [40]. 0.20 g Fe_3O_4 particles was treated with 40 mL HCl (0.1 M) aqueous solution by ultrasonication for 10 min, and which were separated and washed with deionized water subsequently. Thereafter, the treated magnetic particles were homogeneously dispersed in a mixture solution including 100 mL ethanol, 20 mL deionized water, 3.0 mL ammonia aqueous solution (28 wt%), and 2.0 mL TEOS. Finally, the above mixing solution was stirred at room temperature for 6 h, and the Fe_3O_4@SiO_2 composites were separated, washed with ethanol and water and dried in vacuum at 60 °C for 12 h.

The second step is synthesis of magnetic FMMS core-shell composites. Typically, 0.75 mmol $MgCl_2 \cdot 6H_2O$ and 10 mmol ammonia chloride were dissolved in 30 mL deionized water, followed by the addition of 0.8 mL ammonia aqueous solution (28 wt %). 0.08 g Fe_3O_4@SiO_2 spheres were dispersed homogeneously in 20 mL deionized water. After the above two solutions were mixed until homogeneous and transferred into a 100 mL Teflon autoclave heated at 160 °C for 30 min under microwave irradiation. The resulting reddish brown samples were washed several times with ethanol and deionized water. Finally, the FMMS core-shell composites were achieved after dried in vacuum at 60 °C for 12 h.

2.3. Characterization of magnetic FMMS core-shell composites

The phase structure was analyzed by X-ray diffraction using $Cu_{K\alpha}$ radiation (XRD, Philips, X'Pert-PRO, Netherlands). The morphology was investigated by field emission scanning electron microscope (FEI, Quanta 200 FEG, USA) and transmission electron microscopy (JEOL, JEM 2010, Japan). The specific surface area determination and pore volume were performed by Brunauer-Emmett-Teller (BET) and Barrett-Joyner-Halenda (BJH) methods (Beckman Coulter, Omnisorp 100CX, USA), respectively. Magnetic measurements were performed with a superconducting quantum interference device (SQUID) magnetometer (Quantum Design, MPMS XL, USA).

2.4. Adsorption and desorption experiment

The adsorption kinetic experiment were implemented with the following conditions: 80 mg of dried FMMS composites were added to 80 mL of 0.50 mM metal ions solution (as Pb^{2+}, Cu^{2+} or Cd^{2+}), and the mixture solution was stirred continuously with a speed of 200 rpm at optimum pH value (pH = 5) under ambient conditions. The pH value was adjusted by 0.10 M HNO_3 or NaOH. A 4 ml of sample was collected from the solution at a given interval time to evaluate the concentration of adsorbed metal ions by an inductively coupled plasma-optical emission spectrophotometer (Thermo Fisher Scientific, ICP 6000, USA). The selective adsorption activity of magnetic FMMS core-shell composites for different heavy metal ions (mixing solution including Pb^{2+}, Cu^{2+}, Cd^{2+}, initial concentration is 0.5 mM) was conducted same as the above.

The adsorption capacity of the adsorbents for the heavy metal ions was calculated according to the following equation (Eq (1)):

$$q_e = \frac{V(C_0 - C)}{m} \quad (1)$$

C_0 is the initial heavy metal ions in the solution (mg L^{-1}), C_e is the equilibrium concentration after adsorption (mg L^{-1}), V is the solution volume (L) and m is the mass of adsorbent (g).

The successive desorption and regeneration process was used to evaluate the recyclability of the FMMS composite. Firstly the FMMS composites were collected from the solution by external magnet and washed with deionized water for several times to remove the loosely attached metal ions onto the surface of the FMMS composites. Thereafter, the FMMS composites were immersed into $MgCl_2$ solution (2.0 M at pH 5.0) for 8 h under stirring to desorbed the metal ions, then further treated with deionized water and reused in the recycled experiment. The adsorption-desorption

process was repeated six times, and the amount of adsorbed and desorbed metal ions was calculated according to Eq (1). All of the experimental data were the averages of duplicate determinations. The relative errors of the data were about 5%.

3. Results and discussion

3.1. Characterization of the FMMS composites

The synthesis of magnetic FMMS core-shell composites is followed two steps. Step 1 involved the formation of Fe_3O_4@SiO_2 core-shell particles through uniform coating a layer of SiO_2 on the surface of Fe_3O_4 composites by a modified Stöber's process [41]. Step 2 is using microwave-assisted hydrothermal processes to form the hierarchical nanostructured shell of magnesium silicate nanosheets. The silica coating acts as not only the template but also the starting material for the hierarchical nanostructured shell. According to our previous report [35], SiO_2 is dissolved to form silicate anions under the alkaline condition and react with Mg^{2+} cations to produce the mesoporous shell of magnesium silicate nanosheets. Finally, the magnetic FMMS core-shell composites were achieved.

The corresponding morphology and structure of the as-prepared FMMS composites were characterized by SEM and TEM. It was found that the FMMS composites were composed of sphere-like particles and the size was around 720 nm, as shown in SEM image of Fig. 1a. A high magnification image (the inset of Fig. 1a) clearly showed that these composites were hierarchical nanostructure and their surfaces were assembled by a large number of intercrossed nanosheets. The TEM image (Fig. 1b) clearly reveals that the FMMS composites have a typical core-shell nanostructure, that magnesium silicate shells encapsulate the Fe_3O_4 core. As shown in Fig. 1c and d, these core-shell composites were porous hierarchical structures with the assembled shell by a large number of 10 nm thick nanosheets, which agreed well with the SEM observation. Moreover, the particle size distribution of FMMS composites and Fe_3O_4 core revealed that the Fe_3O_4 core was about 615 ± 8 nm in size, and the thickness of magnesium silicate shells was 57 ± 5.5 nm, as shown in Fig. S1. To determine the elemental distribution of Si, O, Fe, Mg on the FMMS composites, TEM-EDS mapping was employed to characterize the FMMS composites. As shown in Fig. 2, the Si, O, Fe, Mg atom were uniformly distributed in accordance with the shape of the examined sphere, further confirming the effectively synthesis of the FMMS composites.

The composition and phase structure of the FMMS composites were investigated by XRD analysis as shown in Fig. 3a, together with pristine Fe_3O_4 and Fe_3O_4@SiO_2 for comparison. The peaks of the curve i in Fig. 2a were indexed as the face-centered cubic of Fe_3O_4 phase (JCPDS card 19-629). After coating with silica layer, the diffraction pattern exhibited the broadening peak of amorphous SiO_2 (centered at 23°) and Fe_3O_4 reflections in Fig. 3a (curve ii). As shown from the curve iii in Fig. 3a, it revealed the co-existence of diffraction peaks of Fe_3O_4 and magnesium silicate in the FMMS composite. Due to the strong diffraction peak of Fe_3O_4, only two low intensity peaks of magnesium silicate located at 19.5° and 60.7° were observed in the curve iii. The magnesium silicate was indexed to the magnesium silicate hydroxide hydrate (reported data: JCPDS no. 03-0174) with an ideal chemical formula of $Mg_3Si_4O_{10}(OH)_2$. The apparent broadening peak in around 19.5° indicated the existence of nanoscale crystals and the relatively imperfect degree of crystallinity in the products [35,42].

The specific area and porosity of the magnetic FMMS core-shell composites were determined by nitrogen sorption measurement (Fig. 3b). The N_2 adsorption-desorption isotherms showed that the FMMS composites displayed a typical IV isotherm with an H1-type

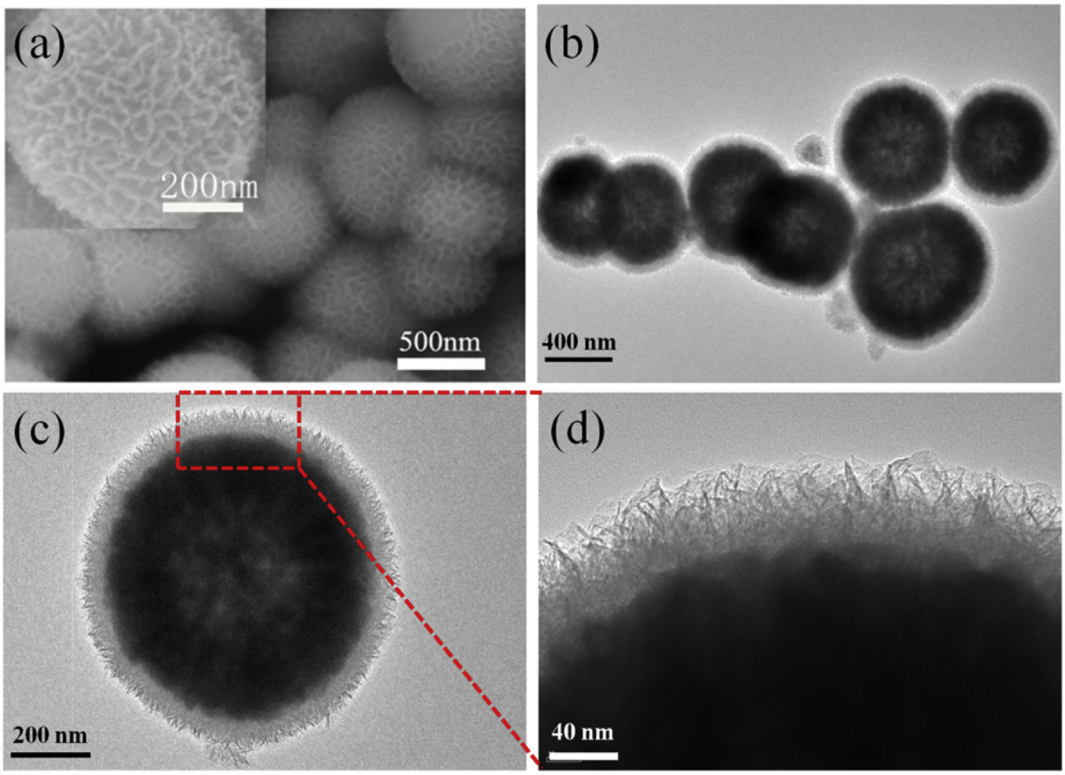

Fig. 1. (a) SEM image and (b) TEM image of the magnetic FMMS core-shell composites, (c) TEM image of single magnetic FMMS core-shell composites, and its magnified TEM image.

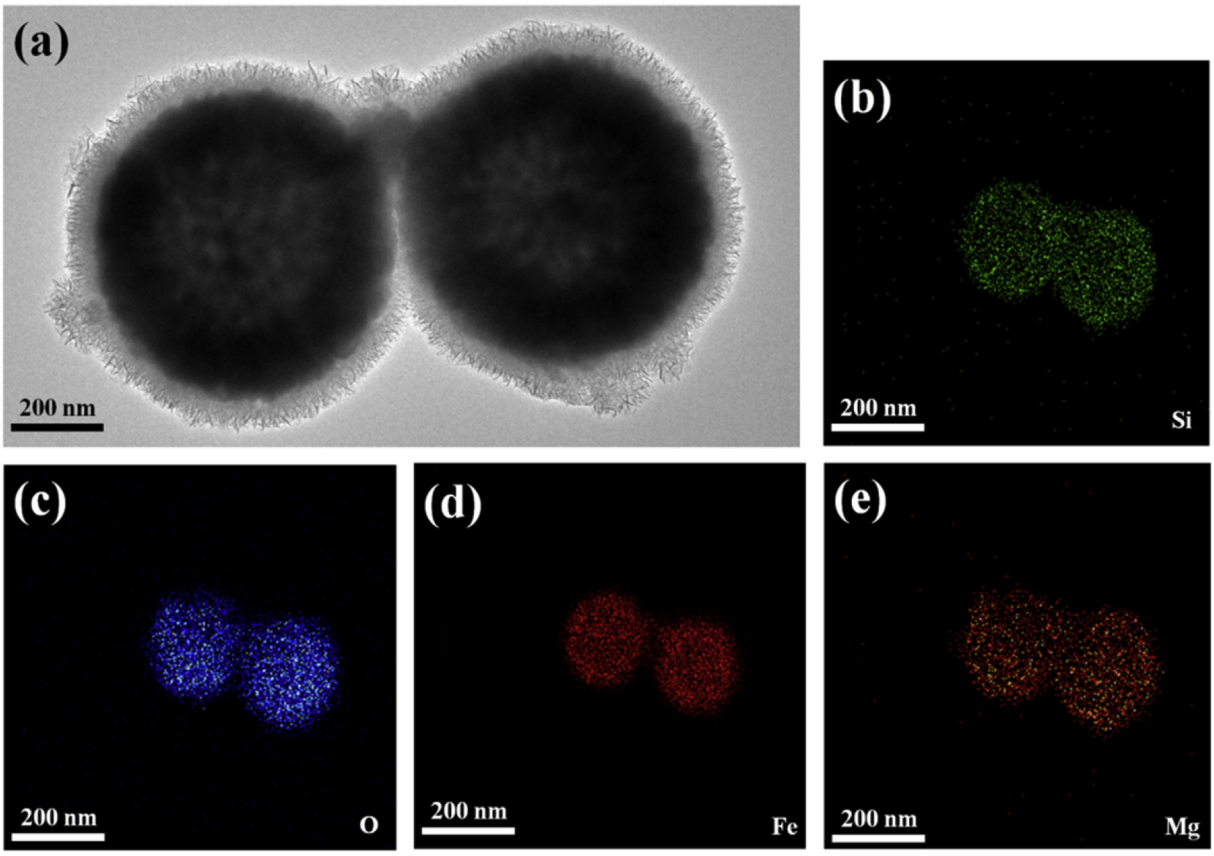

Fig. 2. (a) TEM image of FMMS composites, the element maps of Si (b), O (c), Fe (d) and Mg (e).

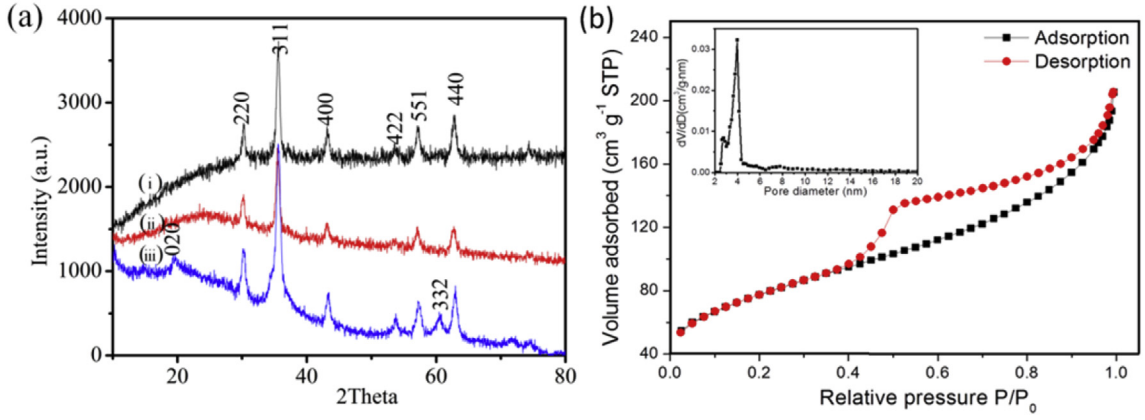

Fig. 3. (a) XRD patterns of (i) Fe_3O_4, (ii) Fe_3O_4@SiO_2, (iii) FMMS composites; (b) N_2 sorption isotherms and pore size distribution (inset) of the FMMS composites.

hysteresis loop at relative pressure of $P/P_0 = 0.40–1.0$. It illuminated that the FMMS composites is representative mesoporous materials, derived from the packing of magnesium silicate nanosheets in the shells. The corresponding BET pore-size distribution curve indicated the uniformed mesoporous with pore diameter of 4.0 nm, as shown in the inset of Fig. 3b. The BET specific area of the obtained core-shell composites was 263.4 m^2/g, which larger than that of Fe_3O_4@SiO_2 (32.9 m^2/g). On the other hand, the space between the magnesium silicate nanosheets in the FMMS composites could be facilitated the fast diffusion of heavy metal ions. Therefore, the mesoporous structures of FMMS composites could increase the amount of surface adsorption active sites and improve the adsorption capacity and rate greatly.

The magnetic hysteresis of FMMS composite was measured using SQUID magnetometer at room temperature (Fig. S2). The applied field was swept between −45 and 45 KOe in the measurement. The hysteresis loop indicated that the FMMS composites exhibited superparamagnetic behavior and its saturation magnetization was 66.5 emu·g^{-1} at room temperature. As shown in inset of Fig. S2, the FMMS composites can be separated using a magnet. After magnetic separation, the FMMS composites were still well dispersed in aqueous solutions.

3.2. Sorption isotherms and thermodynamic parameters

The adsorption isotherms of the FMMS core-shell composites for Cu^{2+} and Pb^{2+} at 293, 303, and 318 K were shown in Fig. 4a and b. With the metal ions concentration increasing, the sorption increased rapidly in the initial stage and then slowly reached equilibrium state. In order to understand the adsorption mechanism and quantify the adsorption capability, two empirical equations, the Langmuir [43] and Freundlich [44] isotherm models, were used to analyze the experimental results. The relative parameters calculated from the two models were listed in Table S1 and the linearized curve-fitting results of Langmuir and Freundlich models were shown in Fig. 5. From the correlation coefficients, it was observed that the Langmuir model agreed well with the experimental data, indicating that the adsorption behavior of Cu^{2+} and Pb^{2+} on the FMMS composites were monolayer adsorption. From Table S1, the maximum adsorption capacity Q_m for Cu^{2+} and Pb^{2+} were 53.5 and 223.2 mg/g at room temperature, respectively. Comparing to the other sorbents, such as MWCNTs (3.439 mg/g for Cu^{2+}, T = 303 K) [45], activated carbon (6.645 and 13.05 mg/g for Cu^{2+} and Pb^{2+}) [46], Mesoporous silicate (24.70 and 19.94 mg/g for Cu^{2+} and Cd^{2+}) [47,48], magnesium silicate hollow nanostructures (60, 71 and 147 mg/g for Cu^{2+}, Cd^{2+} and Pb^{2+}) [49], the magnetic FMMS core-shell composites have excellent removal ability for the heavy metals from wastewater, as shown in Table S5.

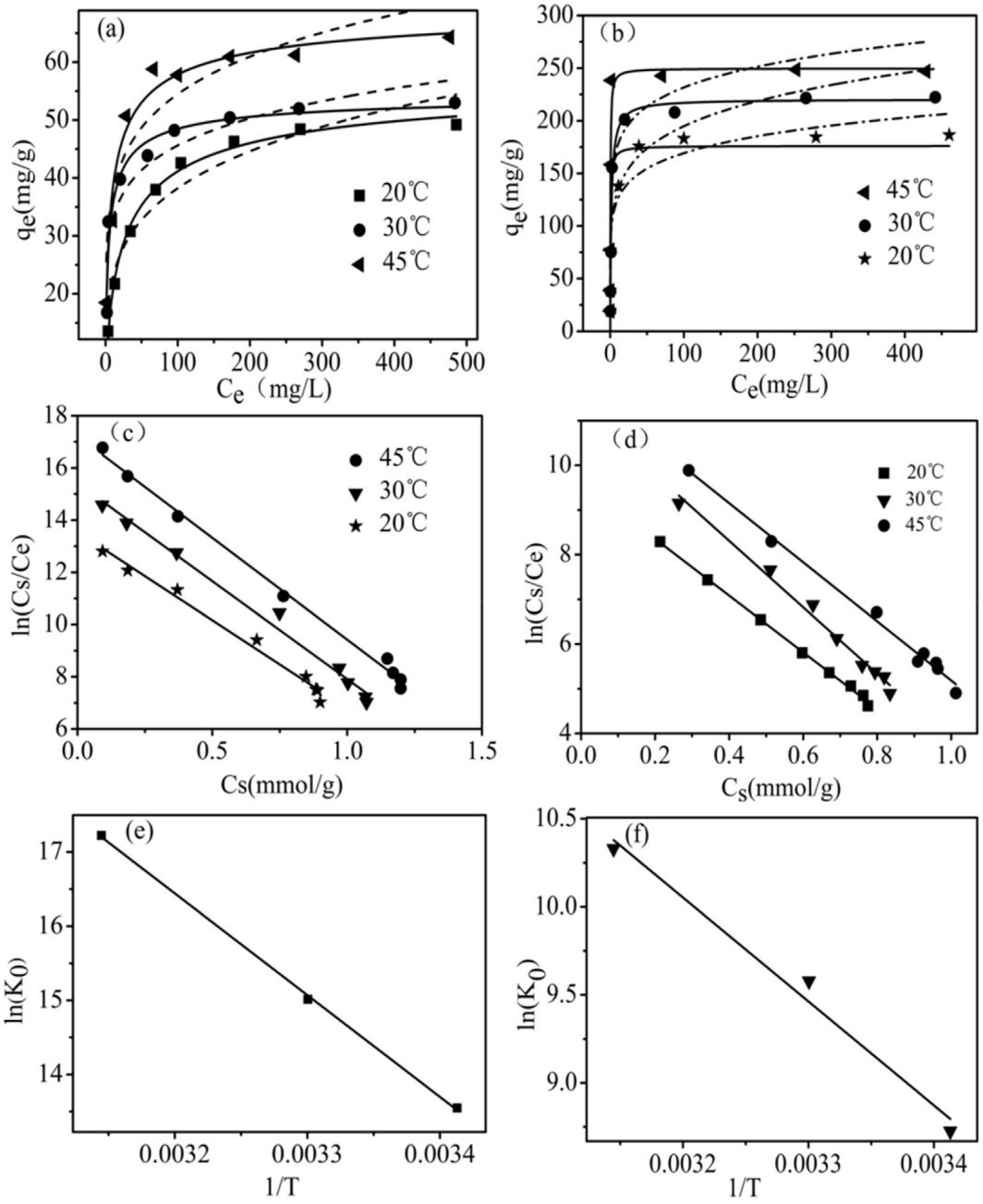

Fig. 4. (a) and (b) are the sorption isotherms, (c) and (d) are the plots of ln (C_S/Ce) as a function C_S, (e) and (f) are the linear plot of lnK_0 vs. *1/T*, for Pb^{2+} and Cu^{2+} adsorbed onto the magnetic FMMS composites at different temperatures, respectively. The concentration of adsorbent is 1 g/L, pH = 5.0, stirring speed = 200 rpm. The solid lines and the dashed lines in (a) and (b) are the Langmuir model simulation and Freundlich model simulation, respectively.

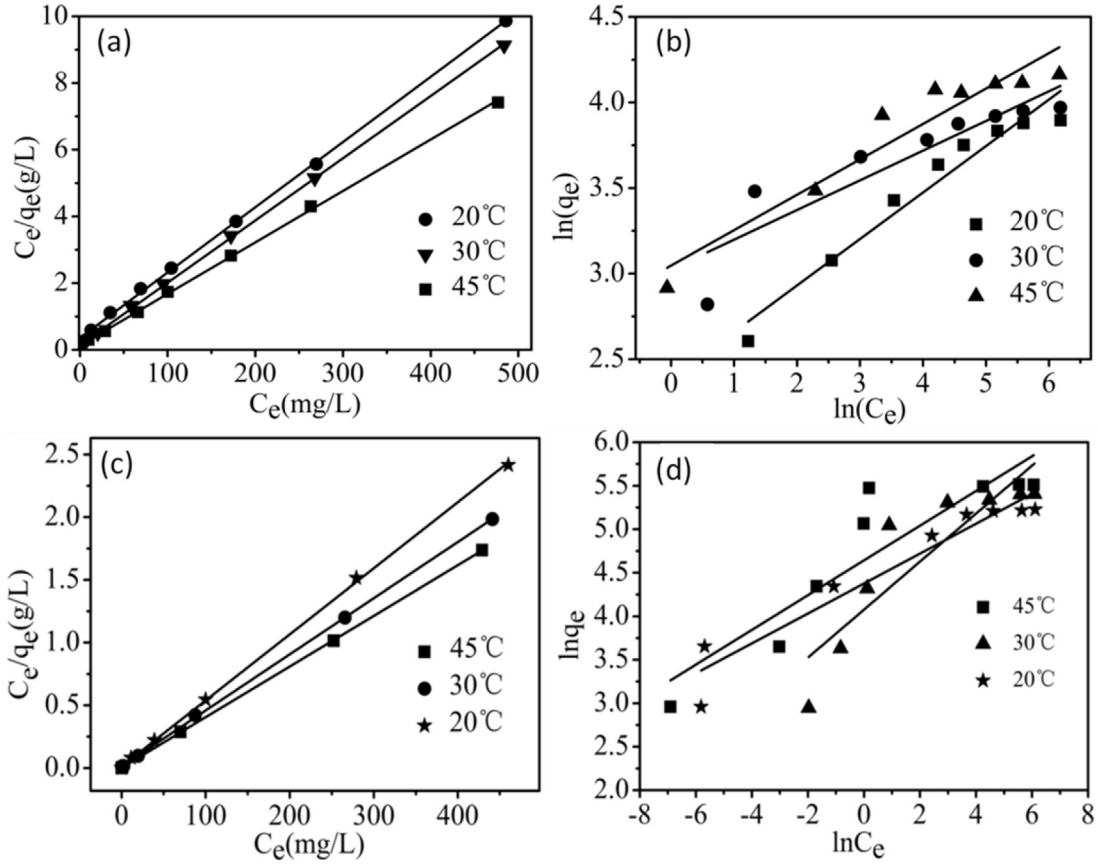

Fig. 5. Linearized (a) Langmuir and (b) Freundlich isotherms for Cu^{2+} adsorption by the FMMS composites at various temperatures; Linearized (c) Langmuir and (d) Freundlich isotherms for Pb^{2+} adsorption by the magnetic FMMS composites at various temperatures.

The adsorption capacity for Pb^{2+} and Cu^{2+} were improved as the increase of temperature, indicating the adsorption process was an endothermic reaction. Thermodynamic parameters were calculated from the thermodynamic equilibrium constant K_0 defined as follows: [50].

$$K_0 = \frac{a_s}{a_e} = \frac{\nu_s}{\nu_e}\frac{C_s}{C_e} \quad (2)$$

a_s is the activity of adsorbed Cu^{2+} or Pb^{2+}, a_e is the activity of Cu^{2+} or Pb^{2+} in solution at equilibrium state, ν_s is the activity coefficient of adsorbed Cu^{2+} or Pb^{2+}, ν_e is the activity coefficient of Cu^{2+} or Pb^{2+} in solution, C_S is the amount of Cu^{2+} or Pb^{2+} adsorbed by per mass of magnetic FMMS core-shell composites (mmol/g) and C_e is the solution concentration of Cu^{2+} or Pb^{2+} at equilibrium state (mmol/mL).

As the concentration of Cu^{2+} and Pb^{2+} in the solution decreased to zero, $\ln K_0$ was calculated by the potting $\ln(C_S/C_e)$ *vs* C_S (Fig. 4c and d) and extrapolating C_S to zero. The gibbs energy (ΔG^0) of adsorption was calculated from the equation: [51,52].

$$\Delta G^0 = -RT \ln K_0 \quad (3)$$

where R is the ideal gas constant (8.3145 J/(mol•K)) and T (K) is the absolute temperature. The standard enthalpy change (ΔH^0) and the standard entropy change (ΔS^0) were calculated from the following equation: [51,52].

$$\ln K_0 = \frac{\Delta S^0}{R} - \frac{\Delta H^0}{RT} \quad (4)$$

Linear plots of $\ln K_0$ *vs* $1/T$ for Cu^{2+} and Pb^{2+} sorption on the FMMS composites were shown in Fig. 4e and f. The calculated values of thermodynamic parameters were listed in Table S2. The negative Gibbs free energy values (ΔG^0) confirmed that adsorption process was a spontaneous under ambient conditions. The values of ΔG^0 at higher temperature were more negative than that at lower temperature, suggesting the more efficient and accessibility adsorption at higher temperature, which is consistent with the observation from Fig. 4. Moreover, Cu^{2+} and Pb^{2+} ions were readily dehydrated at higher temperature, led to the sorption more favorably [52]. The positive values of ΔH^0 for Cu^{2+} and Pb^{2+} suggested an endothermic nature of adsorption. The positive values of ΔS^0 might be due to the release of magnesium ions produced by an ions-exchange reaction between the heavy metal ions and magnesium ions of the magnetic FMMS core-shell composites.

3.3. Adsorption kinetics and competitive adsorption kinetics

The adsorption kinetics of different heavy metal ions (Pb^{2+}, Cd^{2+} and Cu^{2+}) for the magnetic FMMS composites were investigated in order to understand the adsorption behavior of the FMMS composites. Fig. 6a showed the adsorption data of Pb^{2+}, Cd^{2+} and Cu^{2+} ions with different time intervals at 0.5 mM of initial concentration by the magnetic FMMS composites. It was observed that the adsorption rates of Pb^{2+}, Cd^{2+}, and Cu^{2+} were remarkable fast in the initial 30 min and the adsorption equilibrium were achieved within 180 min. The short time period for adsorption equilibrium demonstrated an excellent affinity of the magnetic FMMS composites for the heavy metal ions in aqueous solutions.

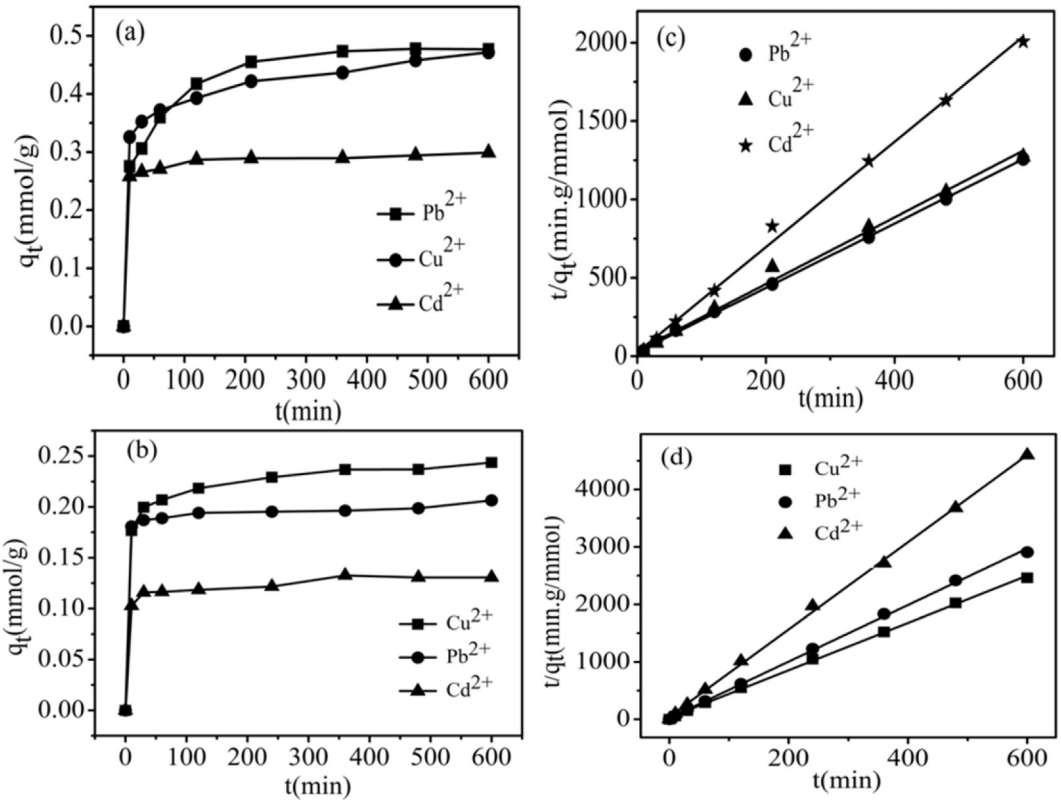

Fig. 6. The removal amount of Pb^{2+}, Cd^{2+} and Cu^{2+} ions by the magnetic FMMS composites (1.0 g L^{-1}) with the duration for 10 h (a) the single ions solution and (b) the mixed ions solution. The initial concentration of Pb^{2+}, Cd^{2+} and Cu^{2+} ions was 0.5 mM. The corresponding pseudo-second-order kinetic plots for the adsorption of Pb^{2+}, Cd^{2+} and Cu^{2+} ions, (c) the single ion solution and (d) the mixed ions solution.

The adsorption kinetics was studied to explain the adsorption mechanism and characteristics of heavy metal ions by the magnetic FMMS composites. The pseudo-second-order model was used to describe the adsorption process: [53,54].

$$\frac{t}{q_t} = \frac{t}{q_e} + \frac{1}{k_2 q_e^2} \tag{5}$$

where q_t (mmol/g) is the adsorption capacity at time t (min), q_e (mmol/g) is the adsorption capacity at adsorption equilibrium; k_2 (g·mmol^{-1}·min^{-1}) is the kinetics rate constants for the pseudo-second-order model. The linear relationship of t/q_t *vs* t was presented in Fig. 6c. The values of k_2 and q_e could be obtained from the slope and intercept of the plot, respectively, which were listed in Table S3a. The pseudo-second-order kinetic model could be satisfactorily used to describe the adsorption behavior of Pb^{2+}, Cd^{2+} and Cu^{2+} on the magnetic FMMS composites in terms of their high correlations ($R^2 > 0.99$). It suggested that the adsorption process of Pb^{2+}, Cd^{2+} and Cu^{2+} on the magnetic FMMS composites involved a chemisorption process by the rate-limiting step [53,55].

In general, waste water contains more than one kind of heavy metal ions. Thus, it is necessary to investigate the competitive adsorption of multiple heavy metal ions in wastewater. In this study, the competitive adsorption kinetics of the mixed system with Pb^{2+}, Cu^{2+} and Cd^{2+} were studied, as shown in Fig. 6b. The linear relationship of t/q_t *vs* t was presented in Fig. 6d. It observed that Cd^{2+} and Pb^{2+} reached the adsorption equilibrium quickly, however, the adsorption of Cu^{2+} was slowly to approach the adsorption equilibrium. The mutual interference effects of metal ions for adsorption were evaluated using q_e'/q_e ratios. The q_e and q_e' represented the adsorption capacity at equilibrium in single and ternary systems, respectively. The value of q_e'/q_e would imply whether the effect of mixing solution of metals was synergistic ($q_e'/q_e > 1$), no interaction ($q_e'/q_e = 1$), or suppressed ($q_e'/q_e < 1$) [53]. The q_e'/q_e values of Cu^{2+}, Pb^{2+} and Cd^{2+} in the ternary system were 0.517, 0.417, and 0.443, respectively. All the values were less than 1, implying that the adsorption of metal ions was suppressed by the presence of other metals in the solution, in other words, there was a competitive adsorption phenomenon between Cu^{2+}, Pb^{2+} and Cd^{2+}. If the metal ions were competing for the same active sites on an adsorbent, those metal ions with a stronger affinity could replace others with a weaker affinity [55]. Therefore, the uptake capacity results (Fig. 6b) revealed that the Cu^{2+} affinity with the magnetic FMMS composites was the strongest among these three metals, followed the order of Cu^{2+}>Pb^{2+}>Cd^{2+}. The selectivity of the adsorbent for different metal ions was associated with the tendency for the metal to hydrolyze, their electronegativity and ionic radium [56,57]. As shown in Table S4, Cu^{2+} possessed a much higher absolute electronegativity than that of Pb^{2+} and Cd^{2+}, suggesting that Cu^{2+} had a stronger attraction than other metal ions to the lone pair of electrons in the oxygen atoms to form more stable complexes. Moreover, Cu^{2+} ions were readily hydrolyzed and favor to interact with the hydroxylated surface. Compared with the radius of Cd^{2+} (9.5 Å) and Pb^{2+} (11.9 Å), the radium of Cu^{2+} of 7.3 Å was very close to that of Mg^{2+} (7.2 Å), facilitating the occurrence of cations exchange. These features could probably well explain the reason that copper ions were selectively adsorbed over other metal ions onto the magnetic FMMS core-shell composites. The above

results were consistent with the literature reports [58,59], the competitive adsorption of heavy metal ions from aqueous solution seemed to be affected by a combination of factors corresponding to the physicochemical characteristics of the magnetic FMMS composites.

3.4. Selectivity test of the FMMS composites

To investigate the selectivity of FMMS composites for heavy metal ions adsorption, 100 mg FMMS were used to treat a 100 mL mixed metal solution containing Zn^{2+}, Pb^{2+}, Hg^{2+}, Cd^{2+}, Mn^{2+} and Cu^{2+} at 0.5 mM of initial concentration, and the mixture solution was stirred continuously at optimum pH value (pH = 5) with a speed of 200 rpm under ambient conditions. The result is shown in Fig. S3. It can be seen that the uptake of Cu^{2+}, Pb^{2+}, Cd^{2+} and Hg^{2+} on FMMS is as high as 0.25, 0.22, 0.17 and 0.08 mmol/g, respectively, while that of Mn^{2+} and Zn^{2+} ions is less than 0.025 mmol/g. It was demonstrated that the competing ions used in the present study have almost no significant influence on the uptake of Cu^{2+}, Pb^{2+} and Cd^{2+} by the FMMS composites under the experimental conditions used. The result of the selectivity test exhibits the following affinity sequence: Cu^{2+}>Pb^{2+}>Cd^{2+}>Hg^{2+}>Mn^{2+}>Zn^{2+} for FMMS composites. The results, in other words, suggested that FMMS sorbents shows a desirable selectivity for Cu^{2+}, Pb^{2+} and Cd^{2+} ions over a range of competing metal ions.

3.5. Recycle performance of the FMMS composites

Since the adsorption-regeneration of adsorbents still remains a challenging in practical implementation of waste water treatment, it was very important to possess excellent regeneration and recycling performance for the FMMS composites [60]. Therefore, the regeneration ability of the FMMS was examined (the initial concentration of Pb^{2+}, Cd^{2+} or Cu^{2+} in the treatment cycles: 0.5 mM, adsorbent loading 100 mg per 60 mL). For refreshing the adsorbent, the samples of Pb^{2+}, Cd^{2+} or Cu^{2+}-adsorbed on the magnetic FMMS composites were immersed into 20 mL $MgCl_2$ (2 M, pH = 5.0) at room temperature under stirring. As shown in Fig. 7, the magnetic FMMS composites showed an adsorption capacity percentage of 99% for Cu^{2+}, 98.5% for Pb^{2+} and 89.5% for Cd^{2+} at the first cycle, which in accordance with the sorption isotherms in Figs. 4 and 6. It was found that about 90.6% adsorbed Cu^{2+}, 91.2% adsorbed Pb^{2+} and 91.6% adsorbed Cd^{2+} can be released by the $MgCl_2$ eluent, respectively. Then, the separated adsorbent powders were treated with deionized water for several times and were further explored for Cu^{2+}, Cd^{2+} and Pb^{2+} removal in the succeeding cycles. We repeated the above procedure for ten cycles. As shown in Fig. 7, the removal efficiency was reduced quickly in the first five cycles, and then tends to slightly decreasing. This may be attributed to that in the previous cycles a certain amount of adsorption sites were occupied on the surface of FMMS composites. However, it still could be found the removal efficiency of 80% for Cu^{2+}, 75% for Pb^{2+}, 65% for Cd^{2+} in the tenth cycle. The superior adsorption-regeneration properties of the magnetic FMMS composites were attributed to their hierarchical structure with assembled mesoporous shell by a large number of intercrossed magnesium silicate nanosheets. Therefore, the magnetic FMMS composites, which exhibited remarkable adsorption capacity, excellent desorption efficiency, and easy separation, was a promising sorbent material for water decontamination.

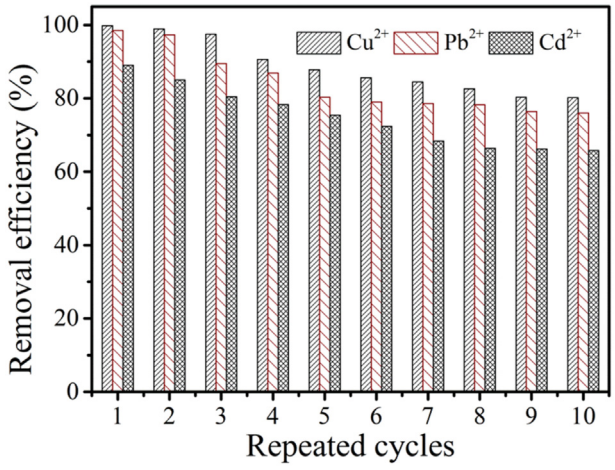

Fig. 7. Removal efficiency of the magnetic FMMS composites for Cu^{2+}, Pb^{2+} and Cd^{2+} under ten time cycles.

3.6. Mesoporous structure and composition-induced enhanced adsorption

To investigate the removal mechanism of the typical magnetic FMMS core-shell composites for heavy metal ions, their morphologies before and after Pb^{2+} ion adsorption were compared. The morphology of the FMMS composite after treatment was examined using SEM (Fig. S4), and an unchanged mesoporous nanostructure was observed after ten cycles, indicating their excellent structural stability. The TEM image (Fig. S5) clearly shows that the assembled magnesium silicate nanosheets features after Pd^{2+} adsorption were still maintained, demonstrated the strong mechanical stability of assembled magnesium silicate nanosheets.

The adsorption behavior of Cu^{2+}, Pd^{2+} and Cd^{2+} ions is largely depend on the surface property, and structure, crystallinity, particle size and surface energy of the adsorbents such as metal ions. In our case, the enhanced adsorption ability for the FMMS composites could mainly be attributed to its mesoporous structure and high specific surface area as well as assembled magnesium silicate nanosheets, as demonstrated in Fig. 3. As mentioned above, the as-synthesized FMMS composites is of large surface area (263.4 m^2/g), much higher than those of the referenced samples Fe_3O_4@SiO_2 (32.9 m^2/g). It is such large surface area and the assembled magnesium silicate nanosheets that FMMS composites possess much more heavy metal ions adsorption sites than that of the as-prepared Fe_3O_4@SiO_2, and hence exhibits significantly enhanced adsorption to Cu^{2+}, Pd^{2+} and Cd^{2+} ions. In addition, as mentioned above, the adsorbent affinity order of three metal ions by FMMS composites is Cu^{2+}>Pb^{2+}>Cd^{2+}, which was associated with the tendency for the metal to hydrolyze, their electronegativity and ionic radium. A possible mechanism for the higher selectivity of Cu^{2+} ions compared to other metal ions is interpreted by considering the great similarity between the ionic radii of Cu^{2+} (0.73 Å) and Mg^{2+} (0.72 Å). This similarity leads to interring of Cu^{2+} ions in the part of the site of Mg^{2+} which may be known as *ion sieve effect*. Such assumption is in agreement with the data reported between Ca^{2+} and Pb^{2+} exchange in the case of calcium phosphate [48] as well as in the case of Cu^{2+} and Mg^{2+} in the case of sepiolite [61]. The adsorption behavior of Cu^{2+}, Pb^{2+} and Cd^{2+}on the FMMS composites was monolayer adsorption with a chemisorption process. The heavy metal ions could not only adsorb on the surface of FMMS composites, but also intercalate into the intercrossed nanosheets of mesoporous magnesium silicate shell, which reveals the synergistic effect of the electrostatic attraction, surface complexation and ion exchange coupled with the adsorption bonding with surface hydroxyl groups.

4. Conclusions

We developed an ultrafast and facile microwave hydrothermal approach to synthesize magnetic FMMS core-shell composites with magnetic Fe_3O_4 cores and hierarchical mesoporous magnesium silicate shells for effective removal of Cu^{2+}, Cd^{2+} and Pb^{2+} from aqueous solutions. The mesoporous structures of the FMMS composites increased the amount of surface active adsorption sites and boosted the adsorption capacity and rate greatly, which exhibited the excellent capability to remove Pb^{2+} (223.2 mg/g) and Cu^{2+} (53.5 mg/g) ions from waste water. The competitive adsorption showed the FMMS composites have good selectivity for Cu^{2+} than the other metal ions, followed the order of Cu^{2+}>Pb^{2+}>Cd^{2+}. The predominant mechanism for the heavy metal cations adsorbed onto the magnetic FMMS composites was the synergistic effect of the electrostatic attraction, surface complexation and ion exchange coupled with the adsorption bonding with surface hydroxyl groups. Furthermore, the FMMS composites exhibited excellent sorption-regeneration performance, which can be easily separated and recovered by external magnet. Thanks to the advantages of high surface area and the high adsorption capacity, the magnetic FMMS core-shell composites show their potential as an attractive adsorbent for the removal of heavy metal ions from industrial waste water.

Acknowledgements

This work was supported by the National Basic Research Program of China (Grant No. 2013CB934302), the Natural Science Foundation of China (Grant No. 51472246 and 21177132), the Anhui Provincial Natural Science Foundation of China (No. 1408085MB39, and 1608085QE89), CAS Key Technology Talent Program and CAS/SAFEA International Partnership Program for Creative Research Teams of Chinese Academy of Sciences, China.

Appendix A. Supplementary data

Supplementary data related to this article can be found at http://dx.doi.org/10.1016/j.micromeso.2017.01.006.

References

[1] U. Forstner, G.T. Wittmann, Metal Pollution in the Aquatic Environment, Springer Science & Business Media, New York, USA, 2012.
[2] J.W. Moore, S. Ramamoorthy, Heavy Metals in Natural Waters: Applied Monitoring and Impact Assessment, Springer Science & Business Media, New York, USA, 2012.
[3] M.Z. Kussainova, R.M. Chernyakova, U.Z. Jussipbekov, S. Pasa, H. Temel, Asia-Pac. J. Chem. Eng. 10 (2015) 833.
[4] X. Xu, G. Duan, Y. Li, G. Liu, J. Wang, H. Zhang, Z. Dai, W. Cai, ACS Appl. Mater. Interfaces 6 (2013) 65.
[5] P. Xu, G.M. Zeng, D.L. Huang, C.L. Feng, S. Hu, M.H. Zhao, C. Lai, Z. Wei, C. Huang, G.X. Xie, Sci. Total Environ. 424 (2012) 1.
[6] C.Y. Cao, J. Qu, W.S. Yan, J.F. Zhu, Z.Y. Wu, W.G. Song, Langmuir 28 (2012) 4573.
[7] M. Hua, S. Zhang, B. Pan, W. Zhang, L. Lv, Q. Zhang, J. Hazard. Mater. 211 (2012) 317.
[8] X. Xin, Q. Wei, J. Yang, L. Yan, R. Feng, G. Chen, B. Du, H. Li, Chem. Eng. J. 184 (2012) 132.
[9] Y. Zhang, Y. Ye, Z. Liu, B. Li, Q. Liu, Q. Liu, X. Li, J. Alloys Compd. 662 (2016) 421.
[10] L. Wang, J. Li, Q. Jiang, L. Zhao, Dalton Trans. 41 (2012) 4544.
[11] I. Ali, M. Asim, T.A. Khan, J. Environ. Manag. 113 (2012) 170.
[12] A.Z. Badruddoza, Z.B.Z. Shawon, W.J.D. Tay, K. Hidajat, M.S. Uddin, Carbohydr. Polym. 91 (2013) 322.
[13] W.W. Tang, G.M. Zeng, J.L. Gong, J. Liang, P. Xu, C. Zhang, B.B. Huang, Sci. Total Environ. 468 (2014) 1014.
[14] V.K. Gupta, O. Moradi, I. Tyagi, S. Agarwal, H. Sadegh, R. Shahryari-Ghoshekandi, A.S.H. Makhlouf, M. Goodarzi, A. Garshasbi, Crit. Rev. Environ. Sci. Technol. 46 (2016) 93.
[15] Y. Zhou, Q. Jin, X. Hu, Q. Zhang, T. Ma, J. Mater. Sci. 47 (2012) 5019.
[16] M. Xie, L. Zeng, Q. Zhang, Y. Kang, H. Xiao, Y. Peng, X. Chen, J. Luo, J. Alloys Compd. 647 (2015) 892.
[17] M. Khajeh, S. Laurent, K. Dastafkan, Chem. Rev. 113 (2013) 7728.
[18] P.Z. Ray, H.J. Shipley, RSC Adv. 5 (2015) 29885.
[19] H. Hu, Z. Wang, L. Pan, J. Alloys Compd. 492 (2010) 656.
[20] F. Liebau, Structural Chemistry of Silicates: Structure, Bonding, and Classification, Springer Science & Business Media, New York, USA, 2012.
[21] H. Manzano, S. Moeini, F. Marinelli, A.C. Van Duin, F.J. Ulm, R.J.M. Pellenq, J. Am. Chem. Soc. 134 (2012) 2208.
[22] Z. Ezzeddine, I. Batonneau-Gener, Y. Pouilloux, H. Hamad, Z. Saad, V. Kazpard, Microporous Mesoporous Mater. 212 (2015) 125.
[23] M.E. Mahmoud, A.E. Abdou, G.M. Nabil, J. Ind. Eng. Chem. 32 (2015) 365.
[24] M. Arshadi, A.R. Faraji, M.J. Amiri, Chem. Eng. J. 266 (2015) 345.
[25] B. Wang, W. Meng, M. Bi, Y. Ni, Q. Cai, J. Wang, Dalton Trans. 42 (2013) 8918.
[26] S. Bhattacharyya, Y. Mastai, R.N. Panda, S.H. Yeon, M.Z. Hu, J. Nanomater 2014 (2014).
[27] J. Ni, L. Zhang, S. Fu, S.V. Savilov, S.M. Aldoshin, L. Lu, Carbon 92 (2015) 15.
[28] M.S. Moorthy, H.B. Kim, A.R. Sung, J.H. Bae, S.H. Kim, C.S. Ha, Microporous Mesoporous Mater. 194 (2014) 219.
[29] G. Qi, X. Lei, L. Li, C. Yuan, Y. Sun, J. Chen, J. Chen, Y. Wang, J. Hao, Chem. Eng. J. 279 (2015) 777.
[30] Q. Ou, L. Zhou, S. Zhao, H. Geng, J. Hao, Y. Xu, H. Chen, X. Chen, Chem. Eng. J. 180 (2012) 121.
[31] C.X. Gui, Q.Q. Wang, S.M. Hao, J. Qu, P.P. Huang, C.Y. Cao, W.G. Song, Z.Z. Yu, ACS Appl. Mater. Interfaces 6 (2014) 14653.
[32] A.G. Sajad, C. Hamida-Tun-Nisa, A. Javid, A. Siraj, Am. J. Anal. Chem. 3 (2012) 18276.
[33] M. Naushad, Z.A. ALOthman, Desalin. Water Treat. 53 (2015) 2158.
[34] B. Lee, Y. Kim, H. Lee, J. Yi, Microporous Mesoporous Mater. 50 (2001) 77.
[35] Y. Wang, G. Wang, H. Wang, C. Liang, W. Cai, L. Zhang, Chem. - Eur. J. 16 (2010) 3497.
[36] S.C. Tang, I.M. Lo, Water Res. 47 (2013) 2613.
[37] J. Chen, F. He, H. Zhang, X. Zhang, G. Zhang, G. Yuan, Ind. Eng. Chem. Res. 53 (2014) 18481.
[38] Y.M. Liu, X.J. Ju, Y. Xin, W.C. Zheng, W. Wang, J. Wei, R. Xie, Z. Liu, L.Y. Chu, ACS Appl. Mater. Interfaces 6 (2014) 9530.
[39] R. Zhao, Y. Wang, X. Li, B. Sun, C. Wang, ACS Appl. Mater. Interfaces 7 (2015) 26649.
[40] H. Deng, X. Li, Q. Peng, X. Wang, J. Chen, Y. Li, Angew. Chem. 117 (2005) 2842.
[41] M. Shao, F. Ning, J. Zhao, M. Wei, D.G. Evans, X. Duan, J. Am. Chem. Soc. 134 (2012) 1071.
[42] Q. Fang, S. Xuan, W. Jiang, X. Gong, Adv. Funct. Mater. 21 (2011) 1902.
[43] D. Xu, X. Tan, C. Chen, X. Wang, J. Hazard. Mater. 154 (2008) 407.
[44] J. Liu, J. Si, Q. Zhang, J. Zheng, C. Han, G. Shao, Ind. Eng. Chem. Res. 50 (2011) 8645.
[45] G. Sheng, J. Li, D. Shao, J. Hu, C. Chen, Y. Chen, X. Wang, J. Hazard. Mater. 178 (2010) 333.
[46] M. Imamoglu, O. Tekir, Desalination 228 (2008) 108.
[47] D.Q. Melo, V.O.S. Neto, J.T. Oliveira, A.L. Barros, E.C.C. Gomes, G.S.C. Raulino, E. Longuinotti, R.F. Nascimento, J. Chem. Eng. Data 58 (2013) 798.
[48] I.M. El-Naggar, M.M. bou-Mesalam, J. Hazard. Mater. 149 (2007) 686.
[49] Y. Zhuang, Y. Yang, G. Xiang, X. Wang, J. Phys. Chem. C 113 (2009) 10441.
[50] H. Genc-Fuhrman, J.C. Tjell, D. McConchie, Environ. Sci. Technol. 38 (2004) 2428.
[51] X.Y. Yu, T. Luo, Y.X. Zhang, Y. Jia, B.J. Zhu, X.C. Fu, J.H. Liu, X.J. Huang, ACS Appl. Mater. Interfaces 3 (2011) 2585.
[52] G. Zhao, J. Li, X. Ren, C. Chen, X. Wang, Environ. Sci. Technol. 45 (2011) 10454.
[53] C. Mahamadi, T. Nharingo, Bioresour. Technol. 101 (2010) 859.
[54] Y.H. Li, Z. Di, J. Ding, D. Wu, Z. Luan, Y. Zhu, Water Res. 39 (2005) 605.
[55] X.S. Wang, H.H. Miao, W. He, H.L. Shen, J. Chem. Eng. Data 56 (2011) 444.
[56] K.K. Choy, G. McKay, Environ. Int. 31 (2005) 845.
[57] D.H. Lee, H. Moon, Korean J. Chem. Eng. 18 (2001) 247.
[58] Y. Xue, H. Hou, S. Zhu, J. Hazard. Mater. 162 (2009) 391.
[59] Y. Zhu, J. Hu, J. Wang, J. Hazard. Mater. 221 (2012) 155.
[60] K.H. Goh, T.T. Lim, Z. Dong, Water Res. 42 (2008) 1343.
[61] L.I. Vico, Chem. Geol. 198 (2003) 213.